Vol 18 No 12, December 2009
1674-1056/2009/18(12)/5552-08

Chinese Physics B

© 2009 Chin. Phys. Soc.
and IOP Publishing Ltd

A new mammalian circadian oscillator model including the cAMP module*

Wang Jun-Wei(王军威)[a)†] and Zhou Tian-Shou(周天寿)[b)]

[a)] *School of Informatics, Guangdong University of Foreign Studies, Guangzhou* 510006, *China*

[b)] *School of Mathematics and Computational Science, Sun Yat-Sen University, Guangzhou* 510275, *China*

(Received 30 March 2009; revised manuscript received 28 April 2009)

In this paper, we develop a new mathematical model for the mammalian circadian clock, which incorporates both transcriptional/translational feedback loops (TTFLs) and a cAMP-mediated feedback loop. The model shows that TTFLs and cAMP signalling cooperatively drive the circadian rhythms. It reproduces typical experimental observations with qualitative similarities, e.g. circadian oscillations in constant darkness and entrainment to light–dark cycles. In addition, it can explain the phenotypes of cAMP-mutant and *Rev-erbα*$^{-/-}$-mutant mice, and help us make an experimentally-testable prediction: oscillations may be rescued when arrhythmic mice with constitutively low concentrations of cAMP are crossed with *Rev-erbα*$^{-/-}$ mutant mice. The model enhances our understanding of the mammalian circadian clockwork from the viewpoint of the entire cell.

Keywords: mammals, circadian clock, cAMP, transcriptional feedback loop

PACC: 8710, 8730E

1. Introduction

In mammals, the suprachiasmatic nucleus (SCN) of the hypothalamus serves as a circadian pacemaker to drive daily rhythms in physiology and behaviour.[1] At the molecular level, the mammalian circadian oscillator is usually modelled by interacting transcriptional/translational feedback loops (TTFLs).[2,3] In these loops, a complex of CLOCK and BMAL1 proteins activates transcription of *periods* (*Per*1, *Per*2 and *Per*3) and *cryptochrome* genes (*Cry*1 and *Cry*2). Following a delay arising from transcriptional and post-translational lags, PER and CRY proteins accumulate as a heteromeric complex in the nucleus to inhibit CLOCK/BMAL1-dependent transcription. The next circadian cycle is initiated once PER/CRY proteins are cleared from the nucleus and thus BMAL1/CLOCK is no longer inhibited. These steps establish a negative transcriptional feedback loop (NTFL) that constitutes the core of the mammalian circadian clock. In a positive transcriptional feedback loop (PTFL), *Bmal*1 transcription is negatively autoregulated by BMAL1 through the REV-ERBα protein. Thus, the PER/CRY complex enhances *Bmal*1 transcription indirectly.[4]

In recent years, several mathematical models have been proposed to better characterize the network underlying mammalian circadian rhythmicity.[5−7] These initial studies provide an important insight into the properties of circadian oscillators. However, recent experimental studies have created additional molecular details that are unaccounted for in the previous models.[8,9] For instance, it was recently observed that the levels of intracellular adenosine 3', 5'-monophosphate (cAMP) in the SCN oscillate in a circadian manner and constitutively low levels of cAMP can eliminate circadian transcription of clock genes, indicating that cAMP is a functional component of the mammalian clockwork.[10,11] Thus, it is necessary to ascertain whether a mathematical model of the current network would provide robust circadian oscillations.

To fill the gap in this area, the present work aims to develop a new theoretical model for the mammalian circadian clock which includes both TTFLs and a cAMP-mediated feedback loop. A reduced but essential set of variables are used to explore the interaction of TTFLs with cAMP signalling and shows that cAMP plays an important role in circadian rhythm generation. In accordance with experimental observations, our model can display stable circadian oscillations in constant darkness (DD) and entrainment of the circa-

*Project supported by the State Key Program of National Natural Science Foundation of China (Grant No 60736028), the National Natural Science Foundation of China (Grant Nos 10871074 and 60704045), and the Research Fund for the Doctoral Program of Higher Education of China (Grant No 20070558053).

†Corresponding author. E-mail: wangjunweilj@yahoo.com.cn

dian oscillator to light–dark (LD) cycles. Except for simulating the phenotypes of cAMP-mutant and *Rev-erbα*-mutant mice, it leads us to an experimentally-testable prediction: oscillations may be rescued when arrhythmic mice with constitutively low concentrations of cAMP are crossed with *Rev-erbα*$^{-/-}$ mutant mice.

2. Development of the mathematical model

The model developed in this paper for the mammalian circadian clock is schematized in Fig.1, whilst the variables representing the concentrations of mRNAs, proteins and cAMP are indicated in parentheses.

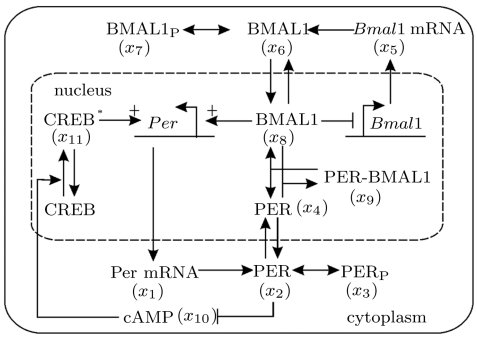


Fig.1. Schematic diagram for the mammalian circadian clock involving both transcriptional regulations of *Per* and *Bmal*1 genes and cytoplasmic cAMP signalling. Variables used in the model are indicated in parentheses.

This model incorporates essential features of molecular processes and describes the interaction between TTFLs and cytoplasmic cAMP signalling. In developing the mathematical model, the following assumptions and their rationale are invoked:

(i) The BMAL1/CLOCK complex activates the expression of *Per*, *Cry* and *Rev-erbα* genes. In our model only the action by BMAL1 is considered because *Clock* expression in mouse SCN is constitutive and *Clock* produces a constant level of CLOCK.[12] In addition, we assume that *Bmal*1 expression is directly, negatively autoregulated by BMAL1 without taking the dynamic *Rev-erbα* gene as an explicit model variable.[3]

(ii) PER and CRY are essential for the maintenance of mammalian rhythms. The knockout of the *Cry*1 or *Cry*2 gene accelerates the rhythmic displaying and delays the periodicity of locomotor activity in DD, respectively.[13] The *Per*2^{Brdm1} mutant mice are initially rhythmic in DD but become arrhythmic.[14] Double mutant mice of *Cry*1$^{-/-}$/*Cry*2$^{-/-}$,[13] *Per*2^{Brdm1}/*Cry*1$^{-/-}$,[15] and *Per*1$^{-/-}$/*Per*2$^{-/-}$[16,17] are immediately arrhythmic in DD. In addition, expressions of *Per* and *Cry* genes are coregulated by the BMAL1/CLOCK complex and the phases of nuclear accumulation PER and CRY proteins are similar.[3] Because of these facts, we represent *Per* and *Cry* mRNAs by a single "lumped" variable "*Per* mRNA", which can be thought of as an average level of *Per* and *Cry* mRNAs. Similarly, PER and CRY proteins are represented by a single variable "PER".

(iii) Although the number of protein phosphorylations that occur may be considerable,[18] single phosphorylated states for PER (PER_P) and BMAL1 ($BMAL1_P$) are assumed in our model. We assume that these phosphorylated proteins are subjected to degradation by enzymes. Such a degradation is also considered for mRNAs, the complex PER-BMAL1, cAMP and phosphorylated CREB.

(iv) By regulating the expression of *Per* genes that contain binding sites for CREB, the cAMP signalling feeds back into the transcriptional cycles.[10] In the model of Fig.1, we assume that cAMP directly activates CREB protein, and phosphorylated CREB then activates transcription of the *Per* gene.

(v) We numerically found that the synthesis of cAMP could be repressed by cytoplasmic PER, or activated by nuclear BMAL1, or others. However, how transcriptional cycles influence oscillations in the concentration of the cytoplsmic cAMP is unclear.[10,11] Here we assume that the cAMP is repressed by protein PER in the cytosol. The results in the following show that such an assumption is in accordance with experiment and thus is reasonable.

Based on the above assumptions, the time evolution for variables in Fig.1 is governed by the following 11 differential equations. For clarity, we group these equations into four categories.

i) *Per* gene expression dynamics: *Per* mRNA (x_1); PER protein in the cytosol (x_2); phosphorylated PER protein in the cytosol (PER_P) (x_3); PER protein in the nucleus (x_4)

$$\frac{\mathrm{d}x_1}{\mathrm{d}t} = v_{per}\frac{(x_8/k_{1per})^m + (x_{11}/k_{2per})^m}{1 + (x_8/k_{1per})^m + (x_{11}/k_{2per})^m} - v_{\mathrm{mp}}\frac{x_1}{k_{\mathrm{mp}} + x_1} - d_1 x_1, \tag{1}$$

$$\frac{\mathrm{d}x_2}{\mathrm{d}t} = v_{\mathrm{PER}}x_1 - T_{1\mathrm{P}}\frac{x_2}{L_{1\mathrm{P}} + x_2} + T_{2\mathrm{P}}\frac{x_3}{L_{2\mathrm{P}} + x_3} - k_{1\mathrm{P}}x_2 + k_{2\mathrm{P}}x_4 - d_2 x_2, \tag{2}$$

$$\frac{\mathrm{d}x_3}{\mathrm{d}t} = T_{1\mathrm{P}}\frac{x_2}{L_{1\mathrm{P}} + x_2} - T_{2\mathrm{P}}\frac{x_3}{L_{2\mathrm{P}} + x_3} - v_{\mathrm{dPC}}\frac{x_3}{L_{\mathrm{d}} + x_3} - d_3 x_3, \tag{3}$$

$$\frac{\mathrm{d}x_4}{\mathrm{d}t} = k_{1\mathrm{P}}x_2 - k_{2\mathrm{P}}x_4 - k_{1\mathrm{PB}}x_4 x_8 + k_{2\mathrm{PB}}x_9 - d_4 x_4. \tag{4}$$

ii) *Bmal*1 gene expression dynamics: *Bmal*1 mRNA (x_5); BMAL1 protein in the cytosol (x_6); phosphorylated BMAL1 protein in the cytosol ($\mathrm{BMAL1_P}$) (x_7); BMAL1 protein in the nucleus (x_8)

$$\frac{\mathrm{d}x_5}{\mathrm{d}t} = v_{bmal1}\frac{k_{bmal1}^n}{k_{bmal1}^n + x_8^n} - v_{\mathrm{mb}}\frac{x_5}{k_{\mathrm{mb}} + x_5} - d_5 x_5, \tag{5}$$

$$\frac{\mathrm{d}x_6}{\mathrm{d}t} = v_{\mathrm{BMAL1}}x_5 - T_{1\mathrm{B}}\frac{x_6}{L_{1\mathrm{B}} + x_6} + T_{2\mathrm{B}}\frac{x_7}{L_{2\mathrm{B}} + x_7} - k_{1\mathrm{B}}x_6 + k_{2\mathrm{B}}x_8 - d_6 x_6, \tag{6}$$

$$\frac{\mathrm{d}x_7}{\mathrm{d}t} = T_{1\mathrm{B}}\frac{x_6}{L_{1\mathrm{B}} + x_6} - T_{2\mathrm{B}}\frac{x_7}{L_{2\mathrm{B}} + x_7} - v_{\mathrm{dBC}}\frac{x_7}{L_{\mathrm{d}} + x_7} - d_7 x_7, \tag{7}$$

$$\frac{\mathrm{d}x_8}{\mathrm{d}t} = k_{1\mathrm{B}}x_6 - k_{2\mathrm{B}}x_8 - k_{1\mathrm{PB}}x_4 x_8 + k_{2\mathrm{PB}}x_9 - d_8 x_8. \tag{8}$$

iii) PER-BMAL1 complex in the nucleus (x_9)

$$\frac{\mathrm{d}x_9}{\mathrm{d}t} = k_{1\mathrm{PB}}x_4 x_8 - k_{2\mathrm{PB}}x_9 - v_{\mathrm{dn}}\frac{x_9}{L_{\mathrm{d}} + x_9} - d_9 x_9. \tag{9}$$

iv) cAMP signalling: cytoplasmic cAMP (x_{10}); phosphorylated CREB ($\mathrm{CREB^*}$) (x_{11})

$$\frac{\mathrm{d}x_{10}}{\mathrm{d}t} = v_{\mathrm{cAMP}}\frac{L_{\mathrm{cAMP}}}{L_{\mathrm{cAMP}} + x_2} - v_{\mathrm{d1}}\frac{x_{10}}{L_{\mathrm{d}} + x_{10}} - d_{10}x_{10}, \tag{10}$$

$$\frac{\mathrm{d}x_{11}}{\mathrm{d}t} = v_{\mathrm{CREB}}\frac{x_{10}}{L_{\mathrm{CREB}} + x_{10}} - v_{\mathrm{d2}}\frac{x_{11}}{L_{\mathrm{d}} + x_{11}} - d_{11}x_{11}. \tag{11}$$

Considering that experimental data for estimating parameter values are largely lacking, we choose these appropriate values by trial-and-error variations to ensure that 1) the model must generate circadian oscillations with a period close to 24 h, 2) the model can correct the phase relationship between mRNAs and proteins, and 3) the model should be able to simulate entrainment to LD cycles. With these considerations, all through this paper we fix the parameter values as follows: $m = 4$, $v_{per} = 1.8\ \mathrm{nMh^{-1}}$, $k_{1per} = 2.5$ nM, $k_{2per} = 2$ nM, $v_{\mathrm{mp}} = 1.1\ \mathrm{nMh^{-1}}$, $k_{\mathrm{mp}} = 0.3$ nM, $v_{\mathrm{PER}} = 0.6\ \mathrm{h^{-1}}$, $T_{1\mathrm{P}} = 1.4\ \mathrm{nMh^{-1}}$, $T_{2\mathrm{P}} = 1.3\ \mathrm{nMh^{-1}}$, $L_{1\mathrm{P}} = 0.1$ nM, $L_{2\mathrm{P}} = 0.1$ nM, $k_{1\mathrm{P}} = 0.4\ \mathrm{h^{-1}}$, $k_{2\mathrm{P}} = 0.2\ \mathrm{h^{-1}}$, $v_{\mathrm{dPC}} = 0.7\ \mathrm{nMh^{-1}}$, $L_{\mathrm{d}} = 0.3$ nM, $k_{1\mathrm{PB}} = 0.5\ \mathrm{nM^{-1}h^{-1}}$, $k_{2\mathrm{PB}} = 0.1\ \mathrm{h^{-1}}$, $n = 2$, $v_{bmal1} = 1\ \mathrm{nMh^{-1}}$, $k_{bmal1} = 2.1$ nM, $v_{\mathrm{mb}} = 0.78\ \mathrm{nMh^{-1}}$, $k_{\mathrm{mb}} = 0.4$ nM, $v_{\mathrm{BMAL1}} = 0.13\ \mathrm{h^{-1}}$, $T_{1\mathrm{B}} = 1.5\ \mathrm{nMh^{-1}}$, $T_{2\mathrm{B}} = 1.1\ \mathrm{nMh^{-1}}$, $L_{1\mathrm{B}} = 0.1$ nM, $L_{2\mathrm{B}} = 0.1$ nM, $k_{1\mathrm{B}} = 0.4\ \mathrm{h^{-1}}$, $k_{2\mathrm{B}} = 0.2\ \mathrm{h^{-1}}$, $v_{\mathrm{dBC}} = 0.5\ \mathrm{nMh^{-1}}$, $v_{\mathrm{dn}} = 0.8\ \mathrm{nMh^{-1}}$, $v_{\mathrm{cAMP}} = 3.8\ \mathrm{nMh^{-1}}$, $L_{\mathrm{cAMP}} = 0.36$ nM, $v_{\mathrm{CREB}} = 1.8\ \mathrm{nMh^{-1}}$, $L_{\mathrm{CREB}} = 0.7$ nM, $v_{\mathrm{d1}} = 0.5\ \mathrm{nMh^{-1}}$, $v_{\mathrm{d2}} = 0.15\ \mathrm{nMh^{-1}}$, $d_j = 0.01\ \mathrm{h^{-1}}$ ($j = 1, 2, \ldots, 9$), $d_{10} = 0.2\ \mathrm{h^{-1}}$ and $d_{11} = 0.5\ \mathrm{h^{-1}}$. It should be noted that except for such a chosen set of parameter values, many other sets of parameter values may yield similar behaviours.

3. Results

3.1. Sustained circadian oscillations under DD

For the given set of parameters, the system displays large-amplitude circadian oscillations of the clock

components, see Fig.2. Figure 2(a) shows the time courses of *Per* and *Bmal*1 mRNA concentrations, whereas the (nonconserved) total amounts of PER and BMAL1 proteins, denoted by $P_{\rm T}$ and $B_{\rm T}$ respectively, and the amounts of cytoplasmic cAMP are plotted separately in Fig.2(b), where $P_{\rm T} = x_2 + x_3 + x_4 + x_9$ and $B_{\rm T} = x_6 + x_7 + x_8 + x_9$. The simulated oscillatory pattern in Fig.2 is stable over time with a period of ∼23.4 h.

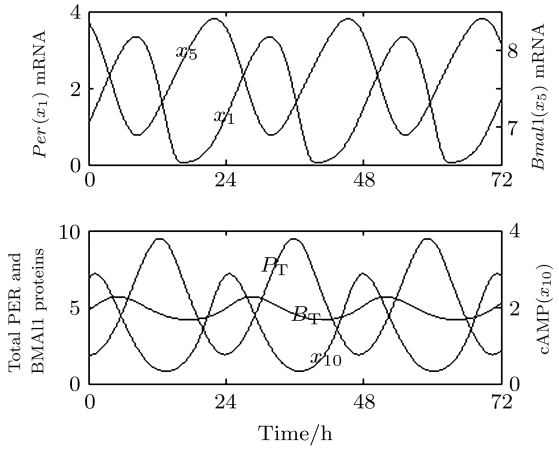


Fig.2. Sustained circadian oscillations for concentrations of mRNAs and proteins, where panel (a) shows time courses of *Per* and *Bmal*1 mRNAs, and panel (b) displays time courses of total amounts of PER and BMAL1 proteins, and cytoplasmic cAMP. The curves are obtained by numerically intergrating Eqs.(1)–(11) for the given parameter values.

At this stage, because no light is incorporated into the model, we define the time at which the concentration of *Per* mRNA reaches 1.2 nM as circadian time (CT) 0 h. In Fig.2(a), the oscillation of *Per* mRNA peaks at the circadian time (CT) ∼8.4 h and is approximately antiphase with respect to that of *Bmal*1 mRNA. *Bmal*1 mRNA bottoms at CT 8.6 h and subsequently peaks at CT 22.1 h, and moreover, its peak precedes the peak of the total BMAL1 protein by about 6.5 h. In contrast, the lag between the peaks of the *Per* mRNA and total amount of PER protein is shorter and about 4 h. These results are consistent with experimental observations that *Per* and *Bmal*1 mRNA levels oscillate almost in antiphase and there exist delays of several hours between *Per* (*Bmal*1) mRNA and PER (BMAL1) protein.[2,3] Figure 2(b) illustrates that the cAMP level oscillates with a high amplitude of about 2.5 nM. Such results hold with the experimental data that the concentration of cAMP in organotypic SCN slice-culture is highly rhythmic.[10]

3.2. Effects of interplay between TTFLs and cAMP signalling

In this subsection, we will investigate the interaction of TTFLs with cAMP signalling. Because PTFL involving the *Rev-erbα* gene is not necessary for rhythm generation,[5,6] we mainly focus on the interplay between NTFL and cAMP signalling. To that end, the strength of NTFL is changed by varying the activation constants k_{1per}, whilst the strength of the cAMP-mediated feedback loop is reflected by varying the activation constants k_{2per}. Note that the strengths of NTFL and cAMP-mediated feedback fall as k_{1per} and k_{2per} rise, respectively.

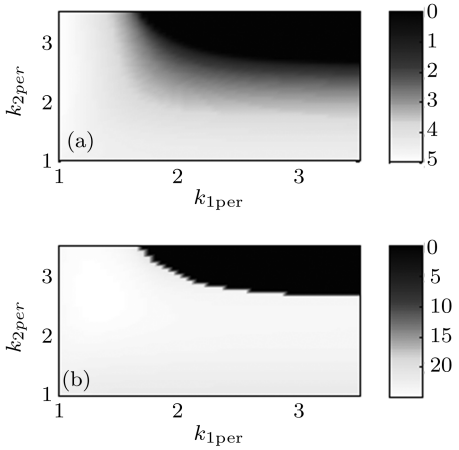


Fig.3. Effect of interplay between TTFLs and cAMP-dependent signalling in the model. Panel (a) shows dependence of the amplitude on the strengths of NTFL (k_{1per}) and cAMP-mediated feedback (k_{2per}), and panel (b) displays dependence of the period on the strengths of NTFL (k_{1per}) and cAMP-mediated feedback (k_{2per}).

Figure 3 depicts the phase diagram in two-dimensional parameter space (k_{1per}, k_{2per}) for the model given in Fig.1, where the dependences of amplitude and period of the system on k_{1per} and k_{2per} are shown in Figs.3(a) and 3(b) respectively. For small values of k_{1per} (e.g., $k_{1per} < 1.65$) which correspond to strong NTFL, the model always exhibits sustained oscillations for $k_{2per} \in (1, 3.5)$, indicating that the TTFLs alone can sustain circadian rhythm. Such a mechanism for mammalian rhythm generation has been modelled previously as an intracellular process.[6–8] We also find that the TTFL-based model alone cannot sustain circadian oscillations in some parameter space (Fig.3). From Fig.3, it can be seen that for both weak NTFL ($k_{1per} > 1.65$) and weak cAMP-mediated feedback ($k_{2per} > 2.65$), the NTFL and cAMP-mediated feedback cooperatively

drive rhythmic oscillations of the SCN, implying that the TTFLs and the cAMP-mediated feedback loops in circadian rhythm generation are functionally non-redundant. These results are consistent with experimental data that the cAMP is a core component of the oscillatory network and the cAMP signals participate in another feedback loop that integrates with TTFLs on clock genes to generate circadian rhythms.[10]

In addition, the effects of changes of k_{1per} and k_{2per} on amplitude and period in our model are non-trivial. Figure 4 illustrates the dependences of the amplitude and the period on k_{2per} (for two typical values of k_{1per}) and k_{1per} (for two typical values of k_{2per}). For a strong NTFL ($k_{1per} = 1.2$), both amplitude and period first become larger and then remain constant with decreasing cAMP-mediated feedback (i.e. k_{2per} rises in value) (see Figs.4(a) and 4(b)). But for a weak NTFL ($k_{1per} = 2.5$), the amplitude monotonically decreases until zero at $k_{2per} = 2.65$, and a local maximum of the period appears at some $k_{2per} \in (1, 2.65)$. It is seen from Figs.4(c) and 4(d) that the amplitude and period changes with k_{1per} (with two fixed parameter values of k_{2per}) exhibit similar behaviours except that they decrease slightly before remaining constant when k_{1per} is increasing for the weak cAMP-mediated feedback loop ($k_{2per} = 1.5$).

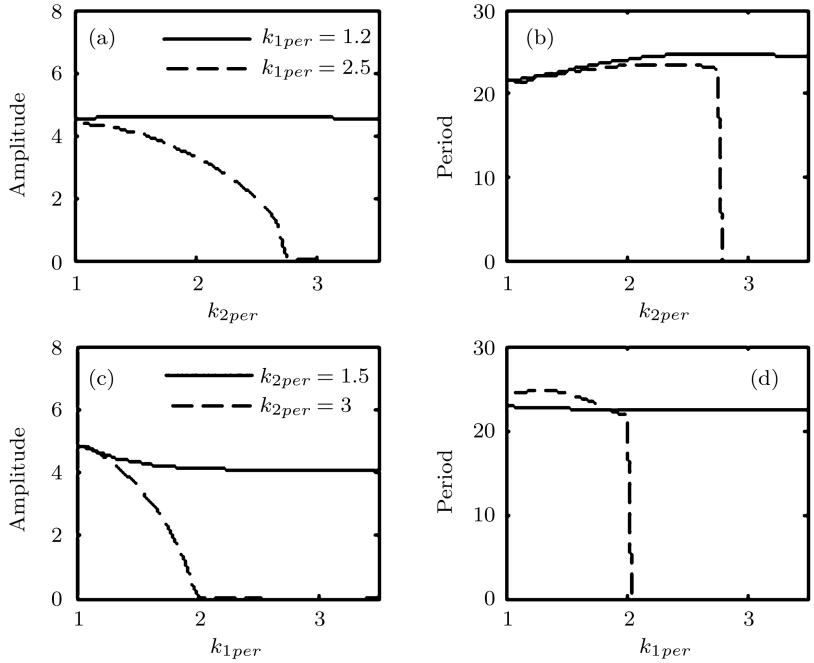


Fig.4. Dependences of amplitude (a) and period (b) of the model on k_{2per} for two fixed parameter values of k_{1per}, and dependences of amplitude (c) and period of model (d) on k_{1per} for two fixed parameter values of k_{2per}.

3.3. Simulation of gene mutant phenotypes

Experiments have shown that reducing cAMP levels by pharmacological means dampens circadian rhythms of clock gene expression.[10] To test whether our model can explain this observation, we create a mathematical mutant which corresponds to mice with a reduced level of cAMP by setting the synthesis rate of cAMP (v_{cAMP} in Eq.(10)) to be 0.2 nMh^{-1}. We assume that there may be other mechanisms contributing to the synthesis of cAMP, so that the parameter v_{cAMP} might remain greater than zero. Figure 5(a) shows that the circadian oscillations have disappeared. Figure 5(b) plots the phenotypes of the *Rev-erbα*$^{-/-}$ mutant mice, where k_{bmal1} is set to be 500 nM such that the effect of the negative feedback of BMAL1 on *Bmal*1 expression is negligible at such a high value of inhibition constant. It can be seen that although *Bmal*1 mRNA is expressed at a constant high level, the *Per* mRNA and the cAMP are rhythmically expressed with a period of about 22.9 h. These results are roughly consistent with reported ob-

servations that in *Rev-erbα*$^{-/-}$ mutant mice, the oscillatory pattern of *Per* mRNA remains stable, although *Bmal*1 mRNA levels do not oscillate but are expressed at constant high levels.[19] In addition, *Rev-erbα* knockout mice display a significantly shorter period than wild-type animals under DD conditions.[19] In the absence of the negative feedback exerted by BMAL1 on the expression of the *Bmal*1 gene, oscillations can be driven by PER/CRY-mediated negative feedback, cAMP-mediated feedback or both. We also find that such oscillations are indeed sustained by PER/CRY-mediated negative feedback as shown in Fig.5(c) where the effect of cAMP-mediated feedback on *Per* expression is negligible at the very low value $v_{\rm cAMP} = 0.1$ nMh^{-1}. This analysis leads to an experimentally testable prediction: circadian oscillations can be rescued when arrhythmic mice with constitutively low concentrations of cAMP by pharmacological means are crossed with *Rev-erbα*$^{-/-}$ mutant mice.

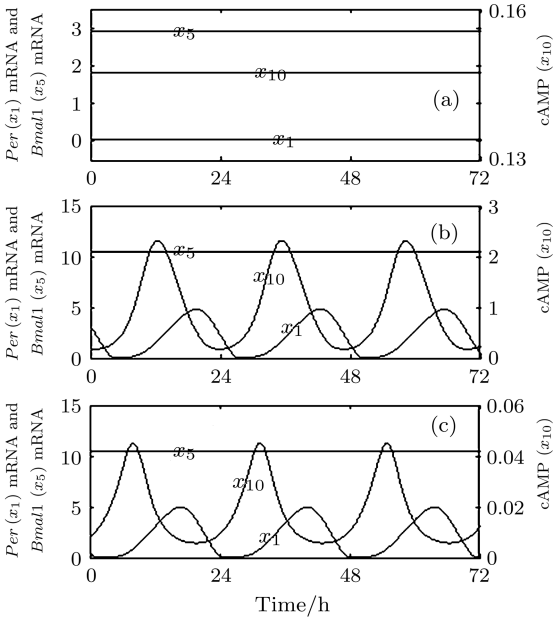


Fig.5. Simulations of phenotypes of cAMP mutant and *Rev-erbα*$^{-/-}$ mutant. Panel (a) shows that sustained oscillations are blocked in the cAMP mutant mice by reducing $v_{\rm cAMP}$ from 3.8 nMh^{-1} to 0.2 nMh^{-1}. Panel (b) exhibits that oscillations are preserved in *Rev-erbα*$^{-/-}$ mutant mice with $k_{bmal1} = 500$ nM, $v_{\rm mb} = 0.93$ nMh^{-1}. Panel (c) displays rescued oscillations of cAMP mutant mice crossed with the *Rev-erbα*$^{-/-}$ mutant mice with $v_{\rm cAMP} = 0.1$ nMh^{-1}, $k_{bmal1} = 500$ nM and $v_{\rm mb} = 0.93$ nMh^{-1}.

3.4. Entrainment to LD cycles

In mammals, light is transmitted to the SCN through the retinohypothalamic tract (RHT), and thus induces acute induction of *Per* expression.[20,21] In terms of modelling, we simulate light exposure by increasing the maximum rate of *Per* expression (v_{per} in Eq.(1)). Consequently, the dynamics of *Per* mRNA is described as

$$\frac{{\rm d}x_1}{{\rm d}t} = (v_{per} + k_{\rm light})\frac{(x_8/k_{1per})^m + (x_{11}/k_{2per})^m}{1 + (x_8/k_{1per})^m + (x_{11}/k_{2per})^m} - v_{\rm mp}\frac{x_1}{k_{\rm mp} + x_1} - d_1 x_1, \quad (1a)$$

where parameter $k_{\rm light}$ denotes the light effect on *Per* gene expression. Figure 6(a) shows the entrainment of circadian oscillations displayed in Fig.2 to an LD cycle. The LD cycle is equally divided into light and dark portions and the period is set to be 24 h, i.e. a 12:12 LD cycle. The parameter $k_{\rm light}$ varies periodically (as a square wave) going from 0 h^{-1} during the dark phase to 0.07 h^{-1} during the light phase. It can be observed that the light phase occurs during the rising portion of *Per* mRNA time course and *Per* mRNA reaches its maximum in the middle of the light phase. The antiphase relationship between *Per* and *Bmal*1 mRNAs is also maintained as in DD. For parameters as in Fig.6(a), we find that the entrainment range appears reasonably broad, i.e. entrainment can occur for an LD cycle length of non-24 h as shown in Fig.6(b) for a 22-h LD cycle, where $k_{\rm light}$ is set to be 0.2 h^{-1}

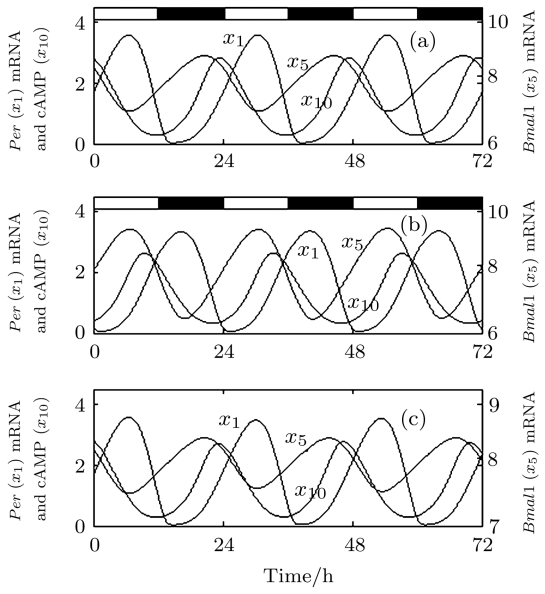


Fig.6. Effects of light on the molecular clocks. Panel (a) shows circadian oscillations after entrainment by a 24-h LD cycle. Panel (b) displays circadian oscillations after entrainment by a non-24 LD cycle, i.e. a 22-h LD cycle. Panel (c) exhibits rhythmic oscillations under conditions of constant light (LL).

during the light phase. By comparing entrained oscillations in Fig.6(a), we observe two interesting points from oscillations entrained by such a non-24 LD cycle. First, the 22-LD cycle alters the phase of the circadian clock such that the maximum of *Per* mRNA appears during the early dark phase. Second, the amplitude of *Per* mRNA (≈ 3.38 nM) becomes smaller. We next simulate constant light (LL) by maintaining k_{light} at its high value $0.07\ \text{h}^{-1}$. The oscillations are still rhythmic but with a period of 23.35 h and an amplitude of 3.48 nM as shown in Fig.6(c), resembling those of the experimental reports.[22]

4. Conclusion and discussion

In the field of mammalian circadian oscillator modelling, our model is unique in the sense that it incorporates the newly found clock component cAMP, except for other core components (e.g. negative elements *Per* and *Cry* genes, positive elements *Bmal*1 and *Clock* genes). In agreement with experimental observations, the model produces 23.4 h sustained oscillations in DD and entrains to both 24 h and non-24 h LD cycles. We have uncovered the novel roles of cytoplasmic cAMP in generating circadian oscillations: they can cooperatively drive circadian oscillations of the SCN. Such functionally non-redundant roles of TTFLs and cAMP-mediated feedback loop may increase the stability of mammalian circadian clocks to environmental changes, such as nutrient condition, metabolic sate of the cell, or redox potential.[23] Our model not only reproduces the phenotypes of several mutants but also predicts that oscillations in arrhythmic mutant mice with constitutively low concentrations of cAMP can be rescued by an additional mutation of *Rev-erbα*.

However, how transcriptional feedback rhythms influence oscillations in the concentration of cytoplsmic cAMP is still an open question.[10,11] The synthesis of cytoplasmic cAMP may be regulated by PER, BMAL1, or other mechanisms, but here we assume that the synthesis of cAMP is repressed by PER in the cytosol. Such an assumption has been shown to be consistent with underlying rules because of successful simulations of the mammalian circadian clock. This suggests that the transcriptional feedback oscillator may influence oscillations of cAMP through the PER protein. Indeed, we have found that the model in which cAMP is repressed by cytosolic BMAL1 exhibits a similar behaviour to that of the present paper (data not shown). Future investigations need to explore the mechanisms through which transcriptional feedback oscillations influence oscillations of cytoplasmic cAMP. Moreover, considering the evidence that cytoplasmic cAMP signalling is involved in VIP-mediated intercellular communication,[24,25] the molecular model proposed here provides a valuable tool to study the questions of coupling and synchronization of networked circadian oscillators at the tissue level.[26−29]

References

[1] Moore R Y, Speh J C and Leak R K 2002 *Cell Tissue Res.* **309** 89

[2] Reppert S M and Weaver D R 2001 *Ann. Rev. Physiol.* **63** 647

[3] Reppert S M and Weaver D R 2002 *Nature* **418** 935

[4] Preitner N, Damiola F, Lopez-Molina L, Zakany J, Duboule D, Albrecht U and Schibler U 2002 *Cell* **110** 251

[5] Leloup J C and Goldbeter A 2003 *Proc. Natl. Acad. Sci.* USA **100** 7051

[6] Becker-Weimann S, Wolf J, Herzel H and Kramer A 2004 *Biophys. J.* **87** 3023

[7] Forger D B and Peskin C S 2003 *Proc. Natl. Acad. Sci.* USA **100** 14806

[8] Lakin-Thomas P L 2006 *J. Biol. Rhythms* **21** 83

[9] Hastings M H, Maywood E S and O'Neill J S 2008 *Curr. Biol.* **18** R805

[10] O'Neill J S, Maywood E S, Chesham J E, Takahashi J S and Hastings M H 2008 *Science* **320** 949

[11] Harrisingh M C and Nitabach M N 2008 *Science* **320** 879

[12] Maywood E S, O'Brien J A and Hastings M H 2003 *J. Neuroendocrinol.* **15** 329

[13] van der Horst G T, Muijtjens M, Kobayashi K, Takano R, Kanno S, Takao M, de Wit J, Verkerk A, Eker A P, van Leenen D, Buijs R, Bootsma D, Hoeijmakers J H and Yasui A 1999 *Nature* **398** 627

[14] Zheng B, Larkin D W, Albrecht U, Sun Z S, Sage M, Eichele G, Lee C C and Bradley A 1999 *Nature* **400** 169

[15] Oster H, Yasui A, van der Horst G T and Albrecht U 2002 *Genes Dev.* **16** 2633

[16] Zheng B, Albrecht U, Kaasik K, Sage M, Lu W, Vaishnav S, Li Q, Sun Z S, Eichele G, Bradley A and Lee C C 2001 *Cell* **105** 683

[17] Bae K, Jin X, Maywood E S, Hastings M H, Reppert S M and Weaver D R 2001 *Neuron* **30** 525

[18] Lee C, Etchegaray J P, Cagampang F R, Loudon A S and Reppert S M 2001 *Cell* **107** 855

[19] Preitner N, Damiola F, Lopez-Molina L, Zakany J, Duboule D, Albrecht U and Schibler U 2002 *Cell* **110** 251

[20] Tischkau S A, Mitchell J W, Tyan S H, Buchanan G F and Gillette M U 2003 *J. Biol. Chem.* **278** 718

[21] Travnickova-Bendova Z, Cermakian N, Reppert S M and Sassone-Corsi P 2002 *Proc. Natl. Acad. Sci.* USA **99** 7728
[22] Ohta H, Yamazaki S and McMahon D G 2005 *Nat. Neurosci.* **8** 267
[23] Rutter J, Reick M and McKnight S L 2002 *Ann. Rev. Biochem.* **71** 307
[24] Yamazaki S, Maruyama M, Cagampang F R and Inouye S T 1994 *Brain Res.* **651** 329
[25] Gerhold L M, Rosewell K L and Wise P M 2005 *J. Neurosci.* **25** 62
[26] Bernard S, Gonze D, Cajavec B, Herzel H and Kramer A 2007 *PLoS Comput. Biol.* **3** e68
[27] To T L, Henson M A, Herzog E D and Doyle F J III 2007 *Biophys. J.* **92** 3792
[28] Wang J W, Zhang J J, Yuan Z J, Chen A M and Zhou T S 2008 *J. Biol. Rhythms* **23** 472
[29] Wang J W, Chen A M, Zhang J J, Yuan Z J and Zhou T S 2009 *Chin. Phys.* B **18** 1294